Synthesis and anti-HIV activity of conformationally restricted bicyclic hexahydroisobenzofuran nucleoside analogs†

Alba Díaz-Rodríguez,[a,b] Yogesh S. Sanghvi,[c] Susana Fernández,[a] Raymond F. Schinazi,[d] Emmanuel A. Theodorakis,*[b] Miguel Ferrero[a] and Vicente Gotor*[a]

Received 22nd October 2008, Accepted 5th January 2009
First published as an Advance Article on the web 11th February 2009
DOI: 10.1039/b818707j

A chiral synthesis of a series of hexahydroisobenzofuran (HIBF) nucleosides has been accomplished *via* glycosylation of a stereo-defined (*syn*-isomer) sugar motif **16** with the appropriate silylated bases. All nucleoside analogs were obtained in 52–71% yield as a mixture of α- and β-anomeric products increasing the breadth of the novel nucleosides available for screening. The structure of the novel bicyclic HIBF nucleosides was established by a single crystal X-ray structure of the β-HIBF thymine analog **22b**. Furthermore, the sugar conformation for these nucleosides was established as N-type. Among the novel HIBF nucleosides synthesized, twenty-five compounds were tested as inhibitor of HIV-1 in human peripheral blood mononuclear (PBM) cells and seven were found to be active (EC_{50} = 12.3–36.2 μM). Six of these compounds were purine analogs with β-HIBF inosine analog **22o** being the most potent (EC_{50} = 12.3 μM) among all compounds tested. The striking resemblance between didanosine (ddI) and **22o** may explain the potent anti-HIV activity.

Introduction

Despite prodigious efforts in combating the HIV infection, it remains the leading cause of death worldwide.[1] Among the various therapeutic treatments available for HIV-1, nucleoside reverse transcriptase inhibitors (NRTIs) has proven to be an important class of drugs with a variety of nucleoside analogs at the forefront. For example, zidovudine (AZT), zalcitabine (ddC), didanosine (ddI), stavudine (d4T, **1** in Fig. 1), lamivudine (3TC), abacavir (ABC), viread (TDF) and emtricitabine (FTC) have been approved by the FDA as anti-HIV drugs.[2] However, the therapeutic potential of these compounds is often compromised by drug resistance and toxicity.[3] In order to overcome these limitations and design improved inhibitors of HIV-1, several investigators[4] have modified the carbohydrate moiety of the nucleosides resulting in enhanced understanding of the structure–activity relationship (SAR).

The anti-HIV studies with various carbohydrate-modified nucleosides have established three salient SAR features that contribute to the observed activity. First, the placement of a 2′,3′-double bond in the structures of d4T (**1**), abacavir, reverset (D-d4FC, **2**) and elvucitabine (L-d4TC) is essential to their anti-HIV-1 activity.[5] For instance, molecular modeling studies with d4T-triphosphate indicate that the double bond is positioned in close proximity to the aromatic side chain of Tyr 115 in the active site of HIV-RT, thus contributing to desirable π–π interactions.[6] Second, the acid labile nature of the 2′,3′-dideoxypurine analogs can be overcome by introducing an electronegative fluorine atom or other hydrophobic groups at the 2′ or 3′-positions (structure **3**) of the carbohydrate moiety.[7] Such groups improve the stability of these compounds at a lower pH and increase their lipophilicity for uptake, both essential features for oral delivery of drugs. Third, nucleoside analogs with a variety of conformational restrictions imposed on the sugar ring (**4**, **5** and **6** in Fig. 1) have resulted in modulation of the enzyme–substrate recognition.[8] In particular, planar pseudo-sugar ring systems are usually preferred. This concept has led to the synthesis of several bicyclic nucleoside analogs with some exhibiting *N*-type (2′-*exo*/3′-*endo*) sugar conformation and antiviral activity.[9]

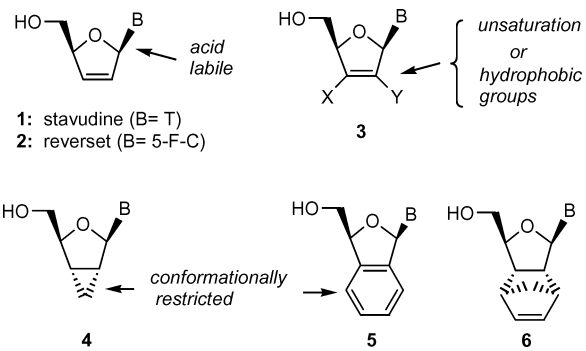

Fig. 1 Designed features of modified nucleosides.

Based on our ongoing interest[10] in the design of conformationally restricted nucleoside analogs for various drug-discovery approaches, we decided to explore the possibility of introducing

[a]*Departamento de Química Orgánica e Inorgánica and Instituto Universitario de Biotecnología de Asturias, Universidad de Oviedo, 33006-Oviedo (Asturias), Spain. E-mail: vgs@uniovi.es; Fax: (+34) 98-510-3448*
[b]*Department of Chemistry and Biochemistry, University of California, San Diego, 9500 Gilman Drive, La Jolla, CA 92093-0358, USA. E-mail: etheodor@ucsd.edu*
[c]*Rasayan Inc., 2802 Crystal Ridge Road, Encinitas, CA 92024-6615, USA*
[d]*Emory University School of Medicine/Veterans Affair Medical Center, Atlanta, Georgia 30033, USA*

† Electronic supplementary information (ESI) available: ^{1}H, ^{13}C NMR spectral data. The level of purity is indicated by the inclusion of copies of ^{1}H, ^{13}C and ^{19}F NMR spectra. In addition, some 2D NMR experiments are shown, which were used to assign the peaks. CCDC reference number 666543. For ESI and crystallographic data in CIF or other electronic format see DOI: 10.1039/b818707j

these three attributes to one molecule and ultimately discover new compounds with antiviral activity. More specifically, we envisioned that a hexahydroisobenzofuran (HIBF) nucleoside, represented by structure **7** (Fig. 2), could contain all three characteristics discussed above. Earlier, it was reported that 3-hydroxymethyl-1,3-dihydrobenzo[*c*]furan nucleosides **5** were found to be inactive as inhibitors of HIV.[11] This lack of activity was attributed to the steric effect of the rigid benzene ring, which reduces the ability of the molecule to access the enzyme-binding site. Replacement of the benzene ring with an HIBF system may offer multiple advantages, such as: (i) possible interactions with Tyr 115 in the active site of HIV-RT due to the 7′–8′ double bond; (ii) stabilization of the glyocosidic linkage at a lower pH due to the C–C bond at the 2′-position; (iii) adoption of the preferred N-type sugar conformation for improved recognition by cellular enzymes, due to the rigid bicyclic motif of HIBF; and (iv) improved lipophilicity for enhanced cellular uptake. With this in mind, we embarked on the synthesis of HIBF type nucleosides.

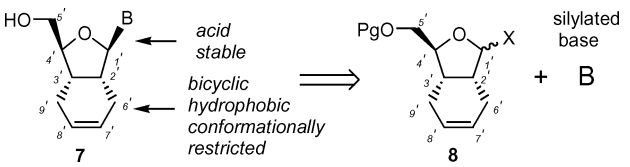

Fig. 2 Concept for the design and synthesis of HIBF nucleosides.

Although many variants of the bicyclic nucleosides have been studied, HIBF nucleosides have not received much attention. As illustrated in Fig. 2, our synthetic approach is based on glycosidation of an appropriately protected HIBF motif **8** with a variety of nucleobases. This strategy is advantageous for a number of reasons. The chirally defined starting material **8** could be synthesized in few steps from inexpensive D-mannitol. The chemically inert HIBF moiety is not expected to interfere in the glycosylation step. The glycosylation reaction would most likely result in the formation of both α- and β-anomers offering both varieties of nucleosides in one step. Appropriately protected **8** could be synthesized in bulk and a large number of nucleoside analogs could be synthesized in parallel mode in a relatively short time. As such, the overall approach is convergent and amenable to scale-up, should any of these nucleosides be required in larger amounts for further studies. Moreover, the HIBF nucleoside family of compounds offers a unique SAR link between the 2′,3′-dideoxynucleosides and the structural requirements for appending a second ring without abolishing the antiviral activity. Herein we report in detail the synthesis of several HIBF nucleosides and their antiviral and cytotoxicity profiles.

It should be noted that while this work was in progress, a communication appeared in the literature[12] describing the synthesis of the uridine analog **7** (B = Uracil). The reported synthesis departs from uridine and employs a ring-closure metathesis reaction to form the cyclohexene ring. As such, this route is not convergent and suffers from a multi-step process that results in the formation of *cis*- and *trans*-isomeric products. Moreover, the biological activities of **7** have not been reported.

Results and discussion

Synthesis of HIBF nucleosides

The bicyclic core of the designed nucleosides was synthesized as shown in Scheme 1. Commercially available D-mannitol was converted to butenolide **10** *via* a sequence of steps that includes: (a) acetonide protection of the 1,2 and 5,6 diol; (b) oxidative cleavage of the 3,4 diol; (c) Wittig olefination of the resulting aldehyde and (d) acid-catalyzed acetonide deprotection and lactonization of the resulting hydroxy ester.[13,14] Initial attempts to silylate butenolide **10** under basic conditions (imidazole, DMAP) led to complete racemization of the starting material, due to the relative acidity of the 4′ hydrogen. However, silylation under acidic conditions (NH_4NO_3, TBDPSCl, DMF)[15] produced the desired compound **11** as a single isomer in excellent yield. The Diels–Alder cycloaddition between **11** and butadiene proceeded exclusively from the opposite face of the bulky TBDPS group and afforded **12** as a single enantiomer in 85% yield.[16] DIBAL-H reduction of lactone **12** proceeded exclusively from the less sterically hindered α-face forming β-lactol **13** in 92% yield.

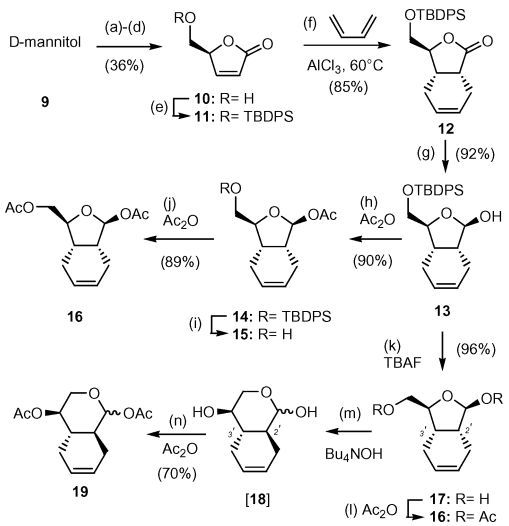

Scheme 1 Synthesis of bicyclic scaffold **16**. *Reagents and conditions:* (a) 0.01 equiv $SnCl_2$, 2,2-dimethoxypropane–DME (2 : 3), reflux, 4 h, 78%; (b) 2.0 equiv $NaIO_4$, sat. aq. $NaHCO_3$–CH_2Cl_2 (1 : 20), 0 °C, 2 h, 73%; (c) 1.5 equiv $Ph_3P{=}CHCO_2Me$, MeOH, 0 °C, 16 h, 70%; (d) conc. H_2SO_4–MeOH (1 : 100), 25 °C, 1 h, 90% (e) 1.2 equiv TBDPSCl, 5.0 equiv NH_4NO_3, DMF, 25 °C, 12 h, 92%; (f) 0.33 equiv $AlCl_3$, CH_2Cl_2, 60 °C, 6 d, 85%; (g) 1.1 equiv DIBAL-H (1 M), CH_2Cl_2, −78 °C 1 h, 92%; (h) 3.0 equiv Ac_2O, pyridine, 25 °C, 12 h, 90%; (i) 1.2 equiv TBAF (1 M), THF, 25 °C, 30 min, 87%; (j) 3.0 equiv Ac_2O, pyridine, 25 °C, 12 h, 89%; (k) 1.2 equiv TBAF (1 M), THF, 25 °C, 25 min, 96%; (l) 4.0 equiv Ac_2O, pyridine, 25 °C, 12 h, 92%; (m) 1.3 equiv Bu_4NOH (33% in H_2O), THF, 25 °C, 6 h; (n) 4.0 equiv of Ac_2O, pyridine, 25 °C, 12 h, 70% (over two steps).

Initially we targeted lactol **13** as the glycosyl donor for coupling with appropriately protected nucleobases. These efforts proved to be unsuccessful, presumably due to the steric hindrance of the bulky TBDPS group. To overcome this problem we decided to change the protecting group at the 5′ center to an acetate functionality. To this end, compound **13** was first acetylated at the C1′ center and then underwent a TBAF-induced desilylation to form alcohol **15** in 78% combined yield. Acetylation of **15** then formed

bicyclic scaffold **16** in 89% yield. Alternatively, desilylation of **13** formed diol **17** that, without further purification, was converted to compound **16** (2 steps, 88% combined yield). It is worth noting that, upon standing, diol **17** can undergo conversion to lactol **18**, in which the C2′ stereocenter was isomerized to form a more stable 6,6 *trans* bicyclic motif. In fact, treatment of **17** under basic conditions (Bu_4NOH, H_2O) followed by acetylation of the reaction mixture led to isolation of diacetate **19** in 70% combined yield.

The glycosidation of diacetate **16** proceeded under Hilbert–Johnson conditions[17] (silylated base, DBU, TMSOTf) to produce a mixture of α- and β-nucleosides in 52–71% overall yield (Scheme 2). The ratio of α/β-anomers was determined by LC-ESI-MS studies used in combination with ^{1}H NMR on the crude reaction mixture. In addition, spectroscopic studies including NOESY measurements confirmed that the β-anomer was the major compound. Unambiguous confirmation of the structure of the synthesized compounds was obtained by a single crystal X-ray analysis of **22b**, the fully deprotected product of **20b** (see Fig. 3).

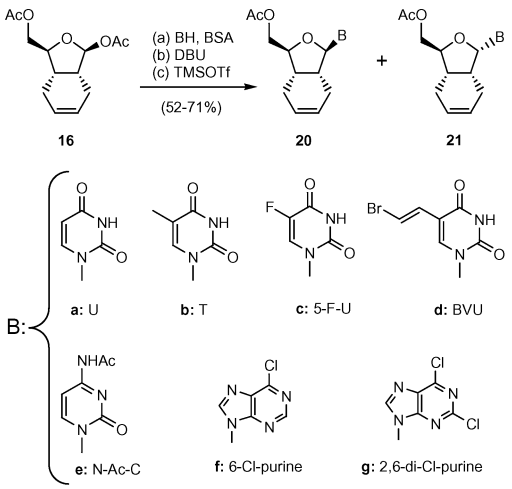

products	a	b	c	d	e	f	g
yield (%) [20+21]	57	65	68	52	55	52	71
ratio (β:α)	1.1:1	1.2:1	only β	1:0.1	1.2:1	1.5:1	2.4:1

Scheme 2 Glycosylation of **16** with pyrimidines and purines. *Reagents and conditions:* (a) 0.5 equiv **16**, 1.0 equiv base, 3.5 equiv BSA, MeCN, 75 °C, 1 h; (b) 1.6 equiv DBU, 25 °C; (c) 3.0 equiv TMSOTf, 0–25 °C, 2–3 h, 52–71% (over three steps).

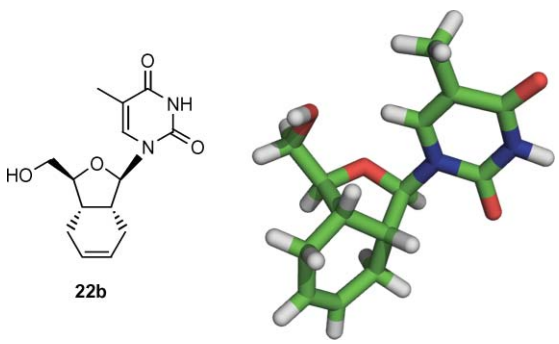

Fig. 3 Single X-ray structure of compound **22b**.

The coupled nucleosides were deprotected under NH_3–MeOH conditions as shown in Scheme 3.[18] We observed that the 5′-acetate

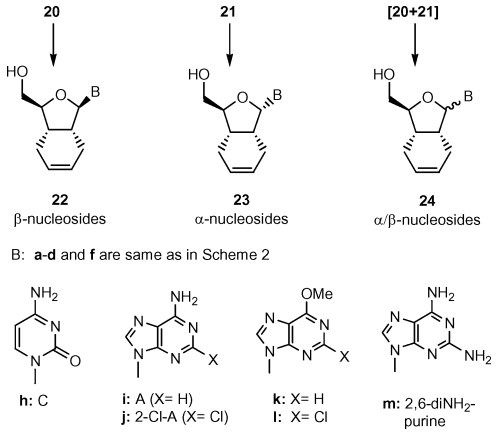

Scheme 3 Deprotection of HIBF nucleosides. *Reagents and conditions:* (a) 2 M NH_3–MeOH, rt for obtaining **a**–**d**, **f**, **h**; (b) NH_3 sat–MeOH, 110 °C for obtaining **i**, **j**, **m**; (c) 2 M NH_3–MeOH, 90–100 °C for obtaining **k**, **l**. Yields are reported in the Experimental section.

group was easily removed in all cases at room temperature. Under these conditions all pyrimidine nucleosides (**20a–e**, **21a–b** and **21d–e**) formed the corresponding 5′-deprotected HIBF nucleosides in excellent yields. These conditions were also successfully used for the selective deprotection of 6-Cl-purine **20f** leading to compound **22f**. However, treatment of **20f** with saturated NH_3–MeOH at 110 °C formed the 6-aminopurine analog **22i**, while under less drastic conditions produced the 6-methoxypurine **22k**.

Treatment of 2,6-dichloropurine **21g** under ammonia led to a mixture of monoamino (**23j**) and diaminopurine derivative (**23m**) in quantitative combined yield. The mixture of compounds **23j** and **23m** was purified by silica gel column chromatography (gradient 50–100% EtOAc–hexane). This transformation is reproducible with both anomeric nucleosides (see Scheme 4).

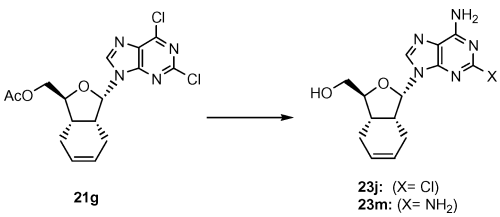

Scheme 4 Synthesis of α-diamino purine bicyclic nucleoside **23**. *Reagents and conditions:* NH_3 sat–MeOH, 110 °C, 36 h, 40% of **23j** and 60% of **23m**.

Alternatively, the diaminopurine **22m** could be obtained by reaction of **20g** with NaN_3 and Me_3P (Scheme 5).[19] Under these conditions the double bond remained unchanged.

The inosine compound **22o** was obtained *via* enzymatic deamination of adenosine analogue **22i** (Scheme 6).[20] This reaction was slower than the reported deamination of natural adenosine and only afforded a 50% yield of the desired product after 72 h. We attribute this sluggish reactivity to the lipophilic nature of the HIBF nucleoside **22i**. Nonetheless, it is remarkable to observe that the presence of the cyclohexene ring is not incompatible to the recognition by the enzyme. The recognition of **22i** as a substrate for adenosine deaminase further confirms that the 5′-hydroxyl group was accessible to the active site in the enzyme for its transformation to **22o**.[21]

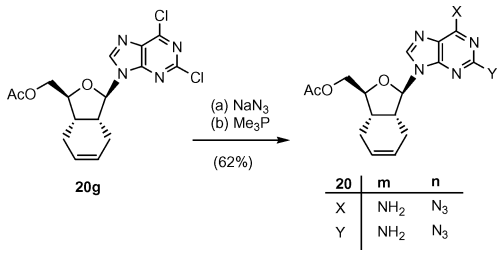

Scheme 5 Purine transformations in β-nucleoside **20g**. *Reagents and conditions:* (a) 4 equiv NaN_3, DMF, 70 °C, 4 h, 80%; (b) 2.2 equiv Me_3P, THF–H_2O (1 : 1), 24 h, 77%.

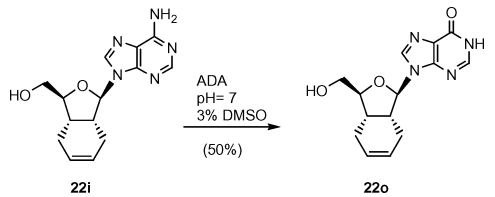

Scheme 6 Synthesis of inosine **22o** through enzymatic deamination. *Reagents and conditions:* 1% ADA, phosphate buffer pH = 7, 3% DMSO, 35 °C, 72 h, 50%.

Single crystal X-ray data for compound **22b** is given in Table 1. HIBF nucleoside analog **22b** crystallized in the form of colorless needles.

Fig. 3 is a PyMOL 0.99[22] drawing, which corresponds to single-crystal X-ray diffraction studies of compound **22b**.[23] Note that the sugar conformation is North type with the 2′-*exo* and 3′-*endo* configurations.

Evaluation of HIBF nucleosides

Acid stability studies. The acid stability of the glycosidic linkage in **22i** (HIBF-ddA) was studied by a direct comparison with 2′,3′-didehydro-2′,3′-dideoxynucleoside (d4A, Fig. 4). The cleavage of the glycosidic bond was studied at pH 2 buffered solution and 37 °C.[24] The degradation of the nucleoside to the free adenine was followed by high performance liquid chromatography (HPLC), where samples were collected at different time points. The data indicated that under experimental conditions d4A was degraded at a significantly faster rate compared to the HIBF nucleoside **22i** ($t_{\frac{1}{2}}$ d4A is about 20 min while $t_{\frac{1}{2}}$ of **22i** is about 6 h). The data confirmed that placement of a C–C bond at the 2′-position enhances significantly the stability of HIBF nucleosides towards lower pH.

Table 1 Crystal data for HIBF nucleoside analog **22b**

Formula	$C_{14}H_{18}N_2O_4$
Molecular weight	278.30
Crystal system	Tetragonal
Space group	$P4_2/n$
a, Å	22.892 (12)
b, Å	22.892 (12)
c, Å	5.224 (4)
Z	8
Final *R*	0.074
Reflections	7109

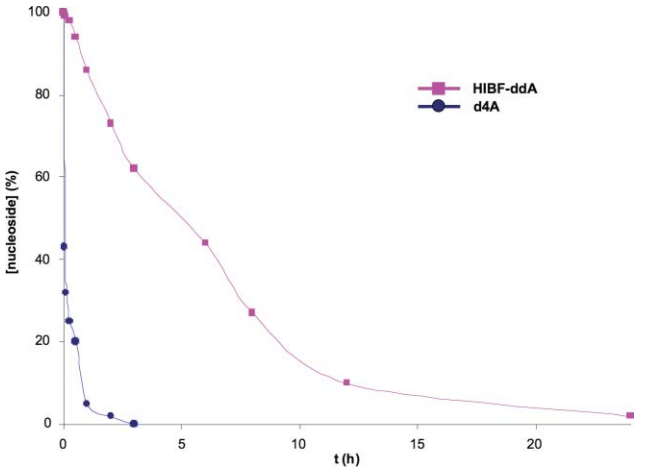

Fig. 4 Percentage *versus* time curves for d4A and HIBF-ddA (**22i**) in pH = 2 buffer at 37 °C.

Biological evaluation

Antiviral assays. A set of twenty-five compounds were tested against HIV-1 (strain LAI) and compared to those of 3′-azido-3′-deoxythymidine (AZT, zidovudine) in an assay with human peripheral blood mononuclear (PBM) cells. Some of the 5′-*O*-acetyl HIBF nucleosides were also included in the testing as potential prodrugs because acyl groups are known to hydrolyze in the presence of cellular esterases generating the free nucleosides. Furthermore, some nucleosides were tested as mixtures of α/β-anomers because these were obtained as an inseparable mixture. A summary of the data, expressed as the effective concentration required to inhibit viral replication by 50% (EC_{50}) and 90% (EC_{90}), is presented in Table 2. HIBF nucleoside analogs **20g/21g**, **22j**, **22l**, **22o**, **23d**, **23f**, and **23j** demonstrate modest activity when compared with the AZT as a control. The potencies (EC_{50}) of the compounds were in the order of **22o** > **22j** > **23d** > **22l** > **20g/21g** > **23f** > **23j**. In general, the purine nucleosides were found to be more potent than the corresponding pyrimidine nucleosides, with the exception of β-5-(2-bromovinyl)uridine **23d**. Among various HIBF purine nucleoside derivatives tested for anti-HIV-1, two α-anomers (6-Cl-purine **23f**, 2-Cl-adenosine **23j**) and a mixture of α/β-anomers (2,6-di-Cl-purines **20g/21g**) also exhibited moderate activities. The HIBF nucleoside **22o** containing the inosine base is the most potent nucleoside analog in this series of compounds (EC_{50} = 12.3 μM). Interestingly, the 2-Cl-adenosine derivative **22j** showed closely related antiviral activity as inosine analog **22o** (EC_{50} 16.5 μM *vs.* 12.3 μM). The similar anti-HIV-1 activities of these two nucleosides could be attributed to possible deamination of the **22j** furnishing a 2-chloro-inosine analog with a close structural resemblance to **22o**. This observation is in agreement with the transformation of the adenosine analog **22i** to **22o** in the presence of adenosine deaminase (Scheme 6). In fact, the masked activity of the inosine analog is also evident in 2-Cl-6-OMe-purine **22l** and 6-Cl-purine **23f**. Both nucleosides could potentially be hydrolyzed under physiological conditions exposing the anti-HIV motif of the 2-chloro-inosine analog and its activity. It is noteworthy that the natural configuration of β-2-Cl-adenine derivative **22j** exhibited 2-fold greater potency than its corresponding α-anomer **23j** (EC_{50} 16.5 μM *vs.* 36.2 μM). Therefore, the observed

Table 2 Effect of analogs against HIV-1 (strain LA1) in human peripheral blood mononuclear (PBM) cells

Analog	Base	Anti-HIV-1 activity in PBM cells[a]		Cytotoxicity (IC_{50}, μM)[b]		
		EC_{50}, μM	EC_{90}, μM	PBM cells	CEM cells	VERO cells
AZT	β-T	0.0015	0.006	> 100	14.3	50.6
20a+21a	α/β-U	60.7	> 100	> 100	> 100	> 100
20b+21b	α/β-T	82.02	> 100	> 100	> 100	> 100
20d+21d	α/β-BVU	> 100	> 100	> 100	> 100	> 100
20e+21e	α/β-N-Ac-C	> 100	> 100	> 100	> 100	> 100
20g+21g	α/β-2,6-di-Cl-purine	24.6	62.4	43.1	5.9	18.9
22a	β-U	90.5	> 100	> 100	67.0	> 100
22b	β-T	> 100	> 100	> 100	> 100	> 100
22c	β-5-F-U	> 100	> 100	> 100	> 100	> 100
22d	β-BVU	77.8	> 100	> 100	> 100	> 100
22f	β-6-Cl-purine	70.3	> 100	> 100	95.6	> 100
22i	β-A	> 100	> 100	> 100	> 100	> 100
22j	β-2-Cl-A	16.5	39.1	27.2	> 100	34.7
22l	β-2-Cl-6-OMe-purine	20.2	95.6	> 100	> 100	76.2
22m	β-2,6-di-NH_2-purine	> 100	> 100	> 100	> 100	> 100
22o	β-I	12.3	44.3	41.4	20.1	50.3
23b	α-T	> 100	> 100	> 100	> 100	> 100
23d	α-BVU	19.0	74.2	31.9	34.2	19.6
23f	α-6-Cl-purine	28.5	46.9	54.2	21.9	98.3
23i	α-A	90.6	> 100	> 100	≥ 100	> 100
23j	α-2-Cl-A	36.2	67.1	30.6	> 100	61.9
23m	α-2,6-di-NH_2-purine	> 100	> 100	≥ 100	> 100	> 100
24b	α/β-T	> 100	> 100	> 100	> 100	> 100
24h	α/β-C	> 100	> 100	> 100	> 100	> 100
24i	α/β-A	> 100	> 100	> 100	> 100	> 100
24j	α/β-2-Cl-A	76.2	> 100	> 100	> 100	> 100

[a] HIV drug susceptibility assay was done as previously described in ref. 25. [b] Cytotoxicity assays in PBM, CEM and Vero cells were done as previously described in ref. 26.

activity of the mixture α/β-2,6-di-Cl-purine **20g/21g** could be due to the presence of β-anomer in the mixture tested. Clearly, there is a correlation between the six active purine nucleoside analogs with the inosine analog being most active. The structural resemblance of the ddI and inosine analog **22o** is remarkable and warrants further studies with the HIBF series of purine nucleosides.

Cytotoxicity assays. The compounds were evaluated for their potential toxic effects on uninfected phytohemagglutinin-stimulated human PBM cells, and also in CEM and Vero (African green monkey kidney) cells. Primary human PBM cells were selected, because these lymphocytes represent slow-growing cells, and were also used in the antiviral assay as host cells. The lymphocytic CEM cells were selected, as they are a continuous nontransformed cell line that replicates quickly and is commonly used for anti-HIV-1 assays. Vero cells were used, as they not only grow rapidly but are also anchored on the surface. The toxicities in these cells may translate into the observed anti-HIV-1 activity. It is noteworthy that the observed cytotoxicity in PBM and CEM cells with inosine analog **22o** could be eliminated by introduction of suitable functionality on the purine ring. For example, β-2-Cl-6-OMe-purine **22l** is not cytotoxic to the PBM and CEM cells. No significant toxicity was detected for most of the compounds devoid of the anti-HIV activity.

In summary, results of both antiviral and cytotoxicity studies indicate that these compounds could offer valuable leads into the development of novel NRTIs with improved therapy for HIV-1 treatment.

Conclusions

In summary, the present study provides for the first time a direct access to a variety of bicyclic nucleoside analogs starting with D-mannitol. The designed HIBF nucleosides contain the three essential SAR elements, which are: (i) the presence of a double bond in the carbohydrate portion of the structure; (ii) the stabilization of the glycosidic linkage at lower pH and (iii) the adoption of a preferred *N*-conformation. The NMR and X-ray studies confirmed that the sugar adopts an *N*-conformation that may be responsible for the observed anti-HIV-1 activity with some of the compounds. The anti-HIV-1 activity exhibited by purine analogs **22o**, **22j** and **22l** is of particular interest because of the close resemblance with the US FDA approved anti-HIV-1 drug ddI. Despite the modified bicyclic carbohydrate motif, the adenosine analog **22i** was deaminated with ADA indicating its ability to mimic the natural adenosine. Therefore, it is reasonable to postulate that the observed anti-HIV-1 activity with purine analogs is perhaps dependent on the recognition by cellular ADA. Interestingly, the antiviral activity and cytotoxicity was modulated by the nature of the substituent on the purine ring. The intracellular metabolism of these nucleosides deserves further attention with particular emphasis on specificity for the ADA.

The anti-HIV-1 activity of ddI is due to its transformation to dideoxyadenosine triphosphate, which inhibits the activity of HIV-1 RT by competing with natural substrate, 2′-deoxyadenosine triphosphate as well as by its incorporation into viral DNA causing termination of the viral chain elongation. Based on the observed anti-HIV-1 activity with various purine analogs, we propose that

the HIBF nucleosides are mimics of ddI and exert their activity *via* incorporation into viral DNA. Because these compounds are stable at lower pH, we believe that they could offer superior bioavailability and longer half-life *in vivo* after oral administration. The transformation of some of the lead compounds (*e.g.* **22o**) into their triphosphate analogs is currently under progress for further biological studies. The synthetic methodology described in this study offers a facile and efficient entry into a variety of bicyclic nucleoside analogs with a wider range of therapeutic applications, such as synthesis of novel nucleosides as antiviral compounds and building blocks for the construction of antisense oligonucleotides.

Experimental section

General techniques

All reagents were bought from Aldrich and Acros at highest commercial quality and used without further purification except where noted. Air- and moisture-sensitive liquids and solutions were transferred *via* syringe or stainless steel cannula. Organic solutions were concentrated by rotary evaporation below 45 °C at approximately 20 mmHg. All non-aqueous reactions were carried out under anhydrous conditions using flame-dried glassware within an argon atmosphere in dry, freshly distilled solvents, unless otherwise noted. THF and CH_2Cl_2 were purified by passage through a bed of activated alumina. Pyridine (Py) was distilled from CaH_2 prior to use. Yields refer to chromatographically and spectroscopically (^{1}H NMR) homogeneous materials, unless otherwise stated. Reactions were monitored by TLC carried out on 0.25 mm E. Merck silica gel plates (60F-254) using UV light as visualizing agent and 7% ethanolic phosphomolybdic acid, or *p*-anisaldehyde solution and heat as developing agents. E. Merck silica gel (60, particle size 0.040–0.063 mm) was used for flash chromatography. LC-ESI-MS analyses were carried out in a chromatograph with UV detector at 280 nm using a VYDAC C-18 column, Cat. Number: 218TP54, (4.6 mm × 250 nm); flow 1 mL min^{-1}; r.t.; gradient MeOH–H_2O as eluent. NMR spectra were recorded on Varian Mercury 300, 400 and/or Unity 500 MHz or Bruker AV-400 or 600 MHz instruments and calibrated using residual undeuterated solvent as an internal reference. The following abbreviations were used to explain the multiplicities: s = singlet, d = doublet, t = triplet, q = quartet, m = multiplet, br = broad. IR spectra were recorded on a Nicolet 320 Avatar FT-IR spectrometer and values are reported in cm^{-1} units. Optical rotations were recorded on a Jasco P-1010 polarimeter and values are reported as follows: $[\alpha]_\lambda^T$ (*c*: g/100 mL, solvent). High resolution mass spectra (HRMS) were recorded on a VG 7070 HS mass spectrometer under electron spray ionization (ESI) conditions. X-Ray data were recorded on a Bruker SMART APEX 3 kW Sealed Tube X-ray diffraction system.

The bicyclic motif of the synthetic hexahydroisobenzofuran nucleosides is abbreviated below as HIBF. The assignment of the NMR data is based on the nucleoside numbering (1′–5′) and the second ring as 6′–9′ positions (Fig. 2).

Synthesis of lactone 12. It was obtained following a previously described procedure.[14] R_f (33% hexane–EtOAc): 0.41; $[\alpha]_D^{20} = 19.4$ (*c* 3.40, CH_2Cl_2); IR (film): ν 3070, 3043, 2932, 2857, 1775, 1112, 704 cm^{-1}; MS (ESI$^+$, *m/z*): 407 [(M + H)$^+$, 100%]; Exact mass found for $C_{25}H_{30}O_3Si$: 406.1964.

Synthesis of lactol 13. A solution of **12** (12.8 g, 31.5 mmol) in dry CH_2Cl_2 (150 mL) was cooled to −78 °C under argon and treated with DIBAL-H (35 mL, 35 mmol, 1 M in CH_2Cl_2) for 1 h. The reaction was quenched with MeOH (10 mL) and the solution was brought to r.t. over a 20 min period. Saturated Rochelle salt was added (stirred for 15 min) and the crude product was extracted with EtOAc (4 × 100 mL). Lactol **13** was isolated in 92% yield as yellow oil. R_f (33% hexane–EtOAc): 0.29; $[\alpha]_D^{20} = -16.9$ (*c* 1.9, CH_2Cl_2); MS (ESI$^+$, *m/z*): 409 [(M + H)$^+$, 100%]; Exact mass found for $C_{25}H_{32}O_3Si$: 408.2120.

Synthesis of acetate 14. Lactol **13** (6.65 mmol) was dissolved in pyridine (40 mL) and Ac_2O (1.8 mL, 19.95 mmol) was added dropwise. The reaction was stirred overnight and then quenched with saturated $NaHCO_3$. The solution was extracted with CH_2Cl_2 (3 × 60 mL). The combined organic extracts were dried (Na_2SO_4). The residue was purified by flash chromatography (10% hexane–EtOAc) to obtain **14** (90%). R_f (25% hexane–EtOAc): 0.65; $[\alpha]_D^{20} = 22.8$ (*c* 0.6, $CHCl_3$); IR (film): ν 3069, 3025, 2925, 2849, 1744, 1421, 1226, 1099 cm^{-1}; MS (ESI$^+$, *m/z*): 468 [(M + NH_4)$^+$, 100%], 473 [(M + Na)$^+$, 45], and 489 [(M + K)$^+$, 15].

Synthesis of acetate 15. Compound **14** (3.34 mmol) was dissolved in 60 mL of dry THF and then treated with TBAF (4.3 mL, 4.3 mmol, 1 M in THF). The reaction was kept under argon at r.t. for 30 min. The solution was extracted with EtOAc (3 × 30 mL). The combined organic extracts were dried using Na_2SO_4 and then filtered. The residue was purified by flash chromatography (30% hexane–EtOAc) to give **15** (89%). R_f (EtOAc): 0.74; $[\alpha]_D^{20} = 47.4$ (*c* 0.9, $CHCl_3$); IR (film): ν 3019, 2922, 2845, 1728, 1427, 1369, 1233, 932 cm^{-1}; MS (ESI$^+$, *m/z*): 230 [(M + NH_4)$^+$, 50%], 235 [(M + Na)$^+$, 75], and 251 [(M + K)$^+$, 20].

Synthesis of diacetate 16. A solution of **17** (31 mmol) in pyridine (100 mL) was treated with Ac_2O (12 mL, 124 mmol). The reaction was stirred overnight and quenched with saturated $NaHCO_3$. The solution was extracted with CH_2Cl_2 (4 × 200 mL). The combined organic extracts were dried using Na_2SO_4 and then filtered. The residue was purified by flash chromatography (15% hexane–EtOAc) to afford **16** (93%). R_f (50% EtOAc–hexane): 0.53; $[\alpha]_D^{20} = -21.8$ (*c* 1.9, $CHCl_3$); IR (film): ν 3030, 2918, 2838, 1737, 1641, 1440, 1239, 933 cm^{-1}; MS (ESI$^+$, *m/z*): 272 [(M + NH_4)$^+$, 20%] and 277 [(M + Na)$^+$, 100].

Synthesis of diol 17. Lactol **13** (31.5 mmol) was dissolved in THF (100 mL) under argon and then treated with TBAF (37.8 mL, 37.8 mmol, 1 M in THF) at r.t. for 25 min. The solution was quenched with brine and extracted with EtOAc (3 × 100mL). The residue was chromatographed using a gradient of 30–70% EtOAc–hexane to give **17** (96%). R_f (EtOAc): 0.44; $[\alpha]_D^{20} = -16.9$ (*c* 1.9, CH_2Cl_2); MS (ESI$^+$, *m/z*): 193 [(M + Na)$^+$, 55%].

Synthesis of diacetate 19. A solution of **13** (31.5 mmol) in THF (100 mL) was treated with TBAOH (47.3 mmol, 33% in H_2O) at r.t. for 6 h. Then, solvents were removed *in vacuo*. The orange residue was treated in pyridine (100 mL) with Ac_2O (12 mL, 124 mmol). The reaction was stirred overnight and then quenched with saturated $NaHCO_3$. The solution was extracted with CH_2Cl_2 (4 × 200 mL). The combined organic extracts were dried using Na_2SO_4, and then filtered. The residue was purified by flash

chromatography (20% hexane–EtOAc) to give **19** (70%). R_f (50% EtOAc–hexane): 0.55; IR (film): ν 3026, 2931, 2839, 1734, 1633, 1233, 936 cm^{-1}; MS (ESI^+, m/z): 272 [$(M + NH_4)^+$, 80%] and 277 [$(M + Na)^+$, 100].

General procedure for condensation of diacetate 16 with heterocyclic bases

To a stirred solution of the different bases (1.81 mmol) in dry MeCN (5.0 mL), BSA was added (1.5 mL, 6.338 mmol). The reaction mixture was heated at 70 °C for 1.5 h. To the resulting clear mixture was added at r.t. a solution of diacetate **16** (0.9 mmol) in dry MeCN (3 mL), followed by DBU (0.434 mL, 2.899 mmol). This solution was cooled to 0 °C and then TMSOTf was added dropwise (1.05 mL, 5.798 mmol). The resulting mixtures were stirred for 2–3 h. Each mixture was poured into an ice-cool saturated $NaHCO_3$ solution and extracted with CH_2Cl_2 (3 × 25 mL). Residues were purified by silica gel column chromatography to give **20** and **21** using a gradient of 33–100% EtOAc–hexane.

HIBF-α/β-uracil (20a+21a). R_f (EtOAc): 0.55; $[\alpha]_D^{20} = -23.4$ (c 0.7, $CHCl_3$); IR (KBr): ν 3200, 3032, 2922, 2844, 1743, 1686, 1461, 1271, 1237, 1042, 705 cm^{-1}; MS (ESI^+, m/z): 307 [$(M + H)^+$, 70%], 324 [$(M + NH_4)^+$, 80], and 329 [$(M + Na)^+$, 100]; LC-ESI-MS (UV 280 nm): coupling ratio β/α 1.1 : 1 t_R(min) = 17.46, 17.91; Exact mass found for $C_{15}H_{18}N_2O_5$: 306.1206.

HIBF-α/β-thymine ((20b+21b). R_f (50% hexane–EtOAc): 0.22; $[\alpha]_D^{20} = -41.26$ (c 1.0, $CHCl_3$); IR (KBr): ν 3197, 3032, 2926, 1744, 1684, 1662, 1473, 1271, 1237, 1044 cm^{-1}; MS (ESI^+, m/z): 321 [$(M + H)^+$, 100%], 338 [$(M + NH_4)^+$, 90], and 343 [$(M + Na)^+$, 95]; LC-ESI-MS (UV 280 nm): coupling ratio β/α 1.2 : 1 t_R(min) = 19.11, 19.29; Exact mass found for $C_{16}H_{20}N_2O_5$: 320.1371.

HIBF-β-5-fluorouracil (20c). R_f (50% hexane–EtOAc): 0.29; $[\alpha]_D^{20} = +10.0$ (c 1.3, $CHCl_3$); IR (KBr): ν 3189, 3075, 3044, 2950, 2857, 1718, 1661, 1469, 1262, 1230, 1093, 1064 cm^{-1}; ^{19}F NMR ($CDCl_3$, 282 MHz): δ 167.1; MS (ESI^+, m/z): 325 [$(M + H)^+$, 30%], 342 [$(M + NH_4)^+$, 60], and 347 [$(M + Na)^+$, 100]; LC-ESI-MS (UV 280 nm): t_R(min) = 19.31; Exact mass found for $C_{15}H_{17}FN_2O_5$: 324.1122.

HIBF-β-5-bromovinyluracil (20d). R_f (50% hexane–EtOAc): 0.41; $[\alpha]_D^{20} = -22.3$ (c 0.6, $CHCl_3$); IR (KBr): ν 3424, 2926, 2874, 1793, 1747, 1700, 1472, 1368, 1280, 1166, 1109, 1041 cm^{-1}; MS (ESI^+, m/z): 433 [$(M^{79}Br + Na)^+$, 100%], 435 [$(M^{81}Br + Na)^+$, 97]; Exact mass found for $C_{17}H_{19}BrN_2O_5$: 410.0872.

HIBF-α/β-cytosine (20e+21e). R_f (EtOAc): 0.24; $[\alpha]_D^{20} = -25.8$ (c 0.4, MeOH); MS (ESI^+, m/z): 370 [$(M + Na)^+$, 100%]; LC-ESI-MS (UV 280 nm): coupling ratio β/α 1.2 : 1 t_R(min) = 19.09, 19.63; Exact mass found for $C_{17}H_{21}N_3O_5$: 347.1480.

HIBF-α/β-6-chloropurine (20f+21f). R_f (50% hexane–EtOAc): 0.37; $[\alpha]_D^{20} = -25.8$ (c 1.0, $CHCl_3$); IR (KBr): ν 3389, 2942, 2890, 1708, 1633, 1489, 1245, 1193, 1094, 920 cm^{-1}; MS (ESI^+, m/z): 371 [$(M^{35}Cl + Na)^+$, 100], 373 [$(M^{37}Cl + Na)^+$, 30]; LC-ESI-MS (UV 280 nm): coupling ratio β/α 1.5 : 1 t_R(min) = 21.19, 21.43; Exact mass found for $C_{16}H_{17}ClN_4O_3$: 348.0982.

HIBF-α/β-2,6-dichloropurine (20g+21g). The two anomers were separated. **20g**: R_f (50% hexane–EtOAc): 0.52; $[\alpha]_D^{20} = -7.3$ (c 0.3, $CHCl_3$); IR (KBr): ν 3370, 2940, 2879, 1728, 1627, 1480, 1239, 1190, 1076, cm^{-1}; MS (ESI^+, m/z): 405 [$(M^{35}Cl^{35}Cl + Na)^+$, 100%], 407 [$(M^{35}Cl^{37}Cl + Na)^+$, 80], and 409 [$(M^{37}Cl^{37}Cl + Na)^+$, 10%]; LC-ESI-MS (UV 280 nm): ratio β/α 2.4 : 1 t_R(min) = 23.62, 24.27; Exact mass found for $C_{16}H_{16}Cl_2N_4O_3$: 382.0600.

21g. R_f (50% hexane–EtOAc): 0.52; $[\alpha]_D^{20} = -40.8$ (c 1.3, $CHCl_3$); MS (ESI^+, m/z): 405 [$(M^{35}Cl^{35}Cl + Na)^+$, 100%], 407 [$(M^{35}Cl^{37}Cl + Na)^+$, 80], and 409 [$(M^{37}Cl^{37}Cl + Na)^+$, 10]; LC-ESI-MS (UV 280 nm): coupling ratio β/α 2.4 : 1 t_R(min) = 23.62, 24.27; Exact mass found for $C_{16}H_{16}Cl_2N_4O_3$: 382.0651.

General protocols for deprotection of HIBF nucleoside derivatives 20–21

Method A (deprotection of 5′-OAc group). Nucleoside derivatives **20a–f+21a–f** (0.1 mmol) were dissolved in a 2 M NH_3–MeOH solution (1.5 mL) and stirred at r.t. overnight. Residues were purified by silica gel column chromatography using a gradient of 33–100% EtOAc–hexane. **Method B**. Nucleoside derivatives **20f+21f**, **20g** and **21g** (0.1 mmol) were treated with a NH_3–MeOH saturated solution (1.5 mL) and stirred at 110 °C in a Parr reactor for 36 h. Residues were purified by silica gel column chromatography (gradient 50–100% EtOAc–hexane) obtaining **22i**, **23i** (95–97%), **22j–22m**, **23j–23m** (quantitative combined yield). **Method C**. Nucleoside derivatives **20f** and **20g** (0.11 mmol) were treated with a 2 M NH_3–MeOH solution (1.8 mL) and stirred at 90–100 °C in a Parr reactor for 30 h. Residues were purified by silica gel column chromatography using a gradient 50–100% EtOAc–hexane.

HIBF-β-uracil (22a). From **20a** using Method A. R_f (EtOAc): 0.40; $[\alpha]_D^{20} = +0.7$ (c 0.3, $CHCl_3$); MS (ESI^+, m/z): 287 [$(M + Na)^+$, 100%]; Exact mass found for $C_{13}H_{15}N_2O_4$: 264.1104.

HIBF-β-thymine (22b). From **20b** using Method A. R_f (50% hexane–EtOAc): 0.16; $[\alpha]_D^{20} = -13.6$ (c 0.3, $CHCl_3$); MS (ESI^+, m/z): 301 [$(M + Na)^+$, 100%]; Exact mass found for $C_{14}H_{18}N_2O_4$: 278.1257.

HIBF-β-5-fluorouracil (22c). From **20c** using Method A. R_f (50% hexane–EtOAc): 0.28; $[\alpha]_D^{20} = +28.6$ (c 0.8, $CHCl_3$); IR (KBr): ν 3508, 3448, 3156, 3040, 2925, 2851, 1682, 1652, 1266, 1093, 1066, 1026 cm^{-1}; ^{19}F NMR ($CDCl_3$, 282 MHz): δ 167.0; MS (ESI^+, m/z): 305 [$(M + Na)^+$, 100%]; Exact mass found for $C_{13}H_{15}FN_2O_4$: 282.1014.

HIBF-β-5-bromovinyluracil (22d). From **20d** using Method A. R_f (50% hexane–EtOAc): 0.32; $[\alpha]_D^{20} = -24.8$ (c 0.6, $CHCl_3$); MS (ESI^+, m/z): 369 [$(M^{79}Br + H)^+$, 100%] and 371 [$(M^{81}Br + H)^+$, 96]; Exact mass found for $C_{15}H_{17}BrN_2O_4$: 368.0395.

HIBF-β-6-chloropurine (22f). From **20f** using Method A. R_f (EtOAc): 0.50; $[\alpha]_D^{20} = -37.2$ (c 1.3, $CHCl_3$); MS (ESI^+, m/z): 329 [$(M^{35}Cl + Na)^+$, 100%] and 331 [$(M^{37}Cl + Na)^+$, 20]; Exact mass found for $C_{14}H_{15}ClN_4O_2$: 306.0682.

HIBF-β-6-aminopurine (22i). From **20f** using Method B. R_f (5% CH_2Cl_2–MeOH): 0.20; $[\alpha]_D^{20} = -19.6$ (c 0.8, DMSO); MS (ESI^+, m/z): 288 [$(M + H)^+$, 100%] and 310 [$(M + Na)^+$, 60]; Exact mass found for $C_{14}H_{17}N_5O_2$: 287.0713.

HIBF-β-6-amino-2-chloropurine (22j). From **20g** using Method B. R_f (10% EtOAc–MeOH): 0.44; $[\alpha]_D^{20} = -8.5$

(*c* 0.3, DMSO); MS (ESI$^+$, *m/z*): 322 [($M^{35}Cl$ + H)$^+$, 100%], 324 [($M^{37}Cl$ + H)$^+$, 20], 344 [($M^{35}Cl$ + Na)$^+$, 80], and 346 [($M^{37}Cl$ + Na)$^+$, 10].

HIBF-β-6-methoxypurine (22k). From **20f** using Method C. R_f (EtOAc): 0.39; MS (ESI$^+$, *m/z*): 325 [(M + Na)$^+$, 100%]; Exact mass found for $C_{15}H_{18}N_4O_3$: 302.0774.

HIBF-β-2-chloro-6-methoxypurine (22l). From **20g** using Method C. R_f (EtOAc): 0.44; MS (ESI$^+$, *m/z*): 359 [($M^{35}Cl$ + Na)$^+$, 100%] and 361 [($M^{37}Cl$ + Na)$^+$, 20]; Exact mass found for $C_{15}H_{17}ClN_4O_3$: 336.1102.

HIBF-β-2,6-diaminopurine (22m). From **20g** using Method B. R_f (10% EtOAc–MeOH): 0.17; $[\alpha]_D^{20} = -19.1$ (*c* 2.5, DMSO); MS (ESI$^+$, *m/z*): 303 [(M + H)$^+$, 100%].

HIBF-α-thymine (23b). From **21b** using Method A. R_f (50% hexane–EtOAc): 0.10; $[\alpha]_D^{20} = -34.5$ (*c* 0.3, $CHCl_3$); MS (ESI$^+$, *m/z*): 301 [(M + Na)$^+$, 100%]; Exact mass found for $C_{14}H_{18}N_2O_4$: 278.1260.

HIBF-α-5-bromovinyluracil (23d). From **21d** using Method A. R_f (50% hexane–EtOAc): 0.14; MS (ESI$^+$, *m/z*): 369 [($M^{79}Br$ + H)$^+$, 100] and 371 [($M^{81}Br$ + H)$^+$, 96]; Exact mass found for $C_{15}H_{17}BrN_2O_4$: 368.0874.

HIBF-α-6-chloropurine (23f). From **21f** using Method A. R_f (EtOAc): 0.40; $[\alpha]_D^{20} = -9.7$ (*c* 0.8, $CHCl_3$); MS (ESI$^+$, *m/z*): 329 [($M^{35}Cl$ + Na)$^+$, 100%] and 331 [($M^{37}Cl$ + Na)$^+$, 30]; Exact mass found for $C_{14}H_{15}ClN_4O_2$: 306.0548.

HIBF-α-6-aminopurine (23i). From **21f** using Method B. R_f (5% CH_2Cl_2–MeOH): 0.09; $[\alpha]_D^{20} = -9.6$ (*c* 2.5, MeOH); MS (ESI$^+$, *m/z*): 288 [(M + H)$^+$, 100%] and 310 [(M + Na)$^+$, 60]; Exact mass found for $C_{14}H_{17}N_5O_2$: 287.0772.

HIBF-α-6-amino-2-chloropurine (23j). From **21g** using Method B. R_f (6.6% EtOAc–MeOH): 0.37; $[\alpha]_D^{20} = -25.9$ (*c* 1.0, DMSO); MS (ESI$^+$, *m/z*): 322 [($M^{35}Cl$ + H)$^+$, 100%] and 324 [($M^{37}Cl$ + H)$^+$, 20].

HIBF-α-2,6-diaminopurine (23m). From **21g** using Method B. R_f (10% EtOAc–MeOH): 0.12; $[\alpha]_D^{20} = -59.8$ (*c* 0.8, MeOH); MS (ESI$^+$, *m/z*): 303 [(M + H)$^+$, 100%].

HIBF-α/β-uracil (24a). From **20a**+**21a** using Method A. R_f (EtOAc): 0.40β, 0.36α; MS (ESI$^+$, *m/z*): 287 [(M + Na)$^+$, 100%].

HIBF-α/β-cytosine (24h). From **20h**+**21h** using Method A. R_f (EtOAc–MeOH 10%): 0.20; $[\alpha]_D^{20} = -28.6$ (*c* 0.7, MeOH); MS (ESI$^+$, *m/z*): 264 [(M + H)$^+$, 70%] and 286 [(M + Na)$^+$, 100]; Exact mass found for $C_{13}H_{17}N_3O_3$: 263.1318.

Synthesis of HIBF-β-2,6-diaminopurine (20m). A solution of **20n** (30 mg, 0.076 mmol) in a mixture THF–H_2O was treated with Me_3P (15.4 μL, 0.174 mmol). Immediately, N_2 was given off and the solution became yellowish. The reaction was stirred for 26 h and then solvents were removed. The residue was purified by silica gel chromatography (2–10% MeOH–EtOAc) to give **20m** in 73% yield. R_f (20% EtOAc–MeOH): 0.49; MS (ESI$^+$, *m/z*): 367 [(M + Na)$^+$, 100%].

Synthesis of HIBF-β-2,6-diazidopurine (20n). A solution of **20g** (0.262 mmol, 100 mg) in DMF (1.8 mL) was treated with NaN_3 (1.048 mmol, 68 mg) at 70 °C for 4 h. Solvent was removed and the residue obtained was purified by silica gel flash chromatography (gradient 30–50% EtOAc–hexane) to give **20n** in 76% yield. R_f (50% hexane–EtOAc): 0.47; MS (ESI$^+$, *m/z*): 419 [(M + Na)$^+$, 100%].

Synthesis of HIBF-β-hypoxanthine 22o. Nucleoside **22i** (20 mg, 0.070 mmol) was dissolved in a phosphate buffer pH = 7/3% DMSO (400 μL) and treated with 1 mg of ADA dissolved in that buffer (100 μL). The residue was purified by flash chromatography (gradient 5–20% MeOH–EtOAc) to give **22o** (50%). R_f (10% EtOAc–MeOH): 0.10; MS (ESI$^+$, *m/z*): 289 [(M + H)$^+$, 100%] and 311 [(M + Na)$^+$, 60].

Antiviral assays

The procedures for the antiviral assays in human peripheral blood mononuclear (PBM) cells have been reported previously.[25] Briefly, uninfected phytohemagglutinin-stimulated human PBM cells were infected with HIV-1 (strain LA1) (about 63 000 disintegrations of RT activity per minute per 10^7 cells per 10 ml of medium). The HIBF nucleososide analogs were then added to duplicate or triplicate cultures. Uninfected and untreated PBM cells were grown in parallel at equivalent cell concentrations as controls. The cultures were maintained in a humidified 5% CO_2–95% air incubator at 37 °C for 6 days after infection, at which point all cultures were sampled for supernatant RT activity. The supernatant was clarified, and the viral particles were then pelleted at 40 000 rpm for 30 min by using a rotor and suspended in virus-disrupting buffer. The RT assay was performed in 96-well microdilution plates by using $(rA)_n \cdot (dT)_{12-18}$ as the template primer. The RT results were expressed in disintegrations per minute per millilitre of originally clarified supernatant.

Cytotoxicity assays

The HIBF nucleoside analogs were evaluated for their potential toxic effects on uninfected phytohemagglutinin-stimulated human PBM cells and also in CEM and Vero (African green monkey kidney) cells as described previously.[26] PBM cells were obtained from the whole blood of healthy HIV-1 and hepatitis B virus-seronegative volunteers and collected by single-step Ficoll-Hypaque discontinuous gradient centrifugation. CEM (CEM-CCRF) cells were a T-lymphoblastoid cell line that was obtained from the American Type Culture Collection, Rockville, Md. The CEM cells were maintained in RPMI 1640 medium supplemented with 20% heat-inactivated fetal bovine serum, penicillin (100 U ml^{-1}), and streptomycin (100 mg ml^{-1}). The PBM and CEM cells were cultured with and without drug for 6 days, at which time portions were counted for cell proliferation and viability by the trypan blue exclusion method. Only the effects on cell growth are reported, since these correlated well with cell viability. The toxicity of the compounds in Vero cells was assessed after 3 days of treatment with a hemacytometer.

Acknowledgements

Financial support of this work by the Spanish Ministerio de Educación y Ciencia (MEC) (Project MEC-07-CTQ-61126) is gratefully acknowledged. A. D.-R. thanks MEC for a predoctoral fellowship. We also thank Dr A. G. DiPasquale and Professor

A. L. Rheingold (UCSD X-Ray Facility) for the reported crystallographic studies and Dr Y. Su (UCSD Mass Spectrometry Facility) for mass analysis and the NSF (CHE-0116662, CHE-9709183 and CHE-0741968) for NMR and MS instrumentation grants. R. F. S. is supported in part by NIH grants 5P30-AI-50409 (CFAR), 5R37-AI-041980 and by the Department of Veterans Affairs. We are grateful to Kim L. Rapp and Jason Grier for their excellent technical assistance.

References and notes

1 (*a*) C. D. Meadows and J. Gervay-Hague, *ChemMedChem*, 2006, **1**, 16–29; (*b*) A. S. Fauci, *Science*, 2006, **313**, 409–409.

2 D. Franklin, A. S. Roemer and L. Placidi, The global antiviral therapeutics market, in *Frontiers in Nucleosides and Nucleic Acids*, ed. R. F. Schinazi and D. C. Liotta, IHL Press, 2004, pp. 159–184.

3 (*a*) R. F. Schinazi, B. A. Larder and J. W. Mellors, *Internatl. Antiviral News*, 2000, **8**, 129; (*b*) S. K. Ono, H. Nakane, P. Herdewijn, J. Balzarini and E. De Clercq, *Mol. Pharmacol.*, 1989, **35**, 578–583; (*c*) G. J. Moyle, *Immunol. Infect. Dis.*, 1995, **5**, 170–182.

4 (*a*) J. Wang, Y. Jin, K. L. Rapp, R. F. Schinazi and C. K. Chu, *J. Med. Chem.*, 2007, **50**, 1828–1839; (*b*) F. Casu, M. A. Chiacchio, R. Romeo and G. Gumina, *Curr. Org. Chem.*, 2007, **11**, 999–1016; (*c*) M. J. Kim and M. W. Chun, *Aust. J. Chem.*, 2007, **60**, 291–295; (*d*) H. Sard, *Nucleosides Nucleotides*, 1994, **13**, 2321–2328; (*e*) M. Okabe and R.-C. Sun, *Tetrahedron Lett.*, 1989, **30**, 2203–2206; (*f*) A. R. Beard, P. I. Butler, J. Mann and N. K. Partlet, *Carbohydr. Res.*, 1990, **205**, 87–91; (*g*) J.-C. Wu and J. Chattopadhyaya, *Tetrahedron Lett.*, 1990, **46**, 2587–2592; (*h*) D. F. Ewing, N.-E. Fahmi, C. Len, G. Mackenzie and A. Pranzo, *J. Chem. Soc., Perkin Trans. 1*, 2000, 3561–3565; (*i*) N. Hossain, J. Plavec, C. Thibaudeau and J. Chattopadhyaya, *Tetrahedron*, 1993, **49**, 9079–9088.

5 K. Lee, Y. Choi, G. Gumina, W. Zhou, R. F. Schinazi and C. K. Chu, *J. Med. Chem.*, 2002, **45**, 1313–1320.

6 H. Choo, Y. Chong and C. K. Chu, *Bioorg. Med. Chem. Lett*, 2003, **13**, 1993–1996.

7 (*a*) V. E. Marquez, C. K.-H. Tseng, H. Mitsuya, S. Aoki, J. A. Kelley, H. Ford, J. S. Roth, S. Broder, D. G. Johns and J. S. Driscoll, *J. Med. Chem.*, 1990, **33**, 978–985; (*b*) K. Ruxrungtham, E. Boone, H. Ford, J. S. Drisoll, R. T. Davey and H. C. Lane, *Antimicrob. Agents Chemother.*, 1996, **40**, 2369–2374.

8 P. Russ, P. Schelling, L. Scapozza, G. Folkers, E. De Clercq and V. E. Marquez, *J. Med. Chem.*, 2003, **46**, 5045–5054.

9 (*a*) Y. Choi, C. George, M. J. Comin, J. J. Barchi, Jr, H. S. Kim, K. A. Jacobson, J. Balzarini, H. Mitsuya, P. L. Boyer, S. H. Huges and V. E. Marquez, *J. Med. Chem.*, 2003, **46**, 3292–3299; (*b*) T. R. Webb, S. Mitsuya and S. Broder, *J. Med. Chem.*, 1988, **31**, 1475–1479.

10 (*a*) B. Haly, R. Bharadwaj and Y. S. Sanghvi, *Synlett*, 1996, 687–689; (*b*) Y. S. Sanghvi, P. D. Cook, Carbohydrates: synthetic methods and applications in antisense therapeutics; an overview in *Carbohydrates Modifications in Antisense Research*, ed. Y. S. Sanghvi and P. D. Cook, ACS Symp. Ser., 1994, **580**, 1–23; (*c*) Y. S. Sanghvi, Synthesis of Nitrogen Containing Linkages for Antisense Oligonucleotides, in *Carbohydrate Mimics: Concepts and Methods*, ed. Yves Chapleur, VCH Publication, 1998, pp. 523–36.

11 D. Egron, C. Perigaud, G. Gosselin, A.-M. Aubertin, A. Faraj, M. Selouane, D. Postel and C. Len, *Bioorg. Med. Chem. Lett.*, 2003, **13**, 4473–4475.

12 J. Drone, M. Egorov, W. Hatton, M.-J. Bertrand, C. Len and J. Lebreton, *Synlett*, 2006, 1339–1342.

13 (*a*) C. R. Schmid, J. D. Bryant, M. Dowlatzedah, J. L. Phillips, D. E. Prather, R. D. Shantz, N. L. Sear and C. S. Vianco, *J. Org. Chem.*, 1991, **56**, 4056–4058; (*b*) J. Mann and A. Weymouth-Wilson, *Carbohydr. Res.*, 1991, **216**, 511–515; (*c*) F. Fazio and M. P. Scheider, *Tetrahedron: Asymmetry*, 2000, **11**, 1869–1876.

14 (*a*) T. P. Brady, S. H. Kim, K. Wen and E. A. Theodorakis, *Angew. Chem., Int. Ed.*, 2004, **43**, 739–742; (*b*) T. P. Brady, S. H. Kim, K. Wen, C. Kim and E. A. Theodorakis, *Chem.–Eur. J.*, 2005, **11**, 7175–7190.

15 S. A. Hardinger and N. Wijaya, *Tetrahedron Lett.*, 1993, **34**, 3821–3824.

16 (*a*) R. Casas, T. Parella, V. Branchadell, A. Oliva, R. M. Ortuño and A. Guignant, *Tetrahedron*, 1992, **48**, 2659–2680; (*b*) R. M. Ortuño, M. Ballesteros, J. Corbera, F. Sanchez-Ferrando and J. Font, *Tetrahedron*, 1988, **44**, 1711–1719; (*c*) R. M. Ortuño, J. Corbera and J. Font, *Tetrahedron Lett.*, 1986, **27**, 1081–1084.

17 (*a*) G. E. Hilbert and T. B. Johnson, *J. Am. Chem. Soc.*, 1930, **52**, 4489–4494; (*b*) H. Vorbruggen, C. Ruh-Pohlenz, *Handbook of nucleoside synthesis*, Wiley Interscience, 2001, pp. 10–24.

18 Y. S. Sanghvi, B. K. Bhattacharya, G. D. Kini, S. S. Matsumoto, S. B. Larson, W. B. Jolley, R. K. Robins and G. R. Revankar, *J. Med. Chem.*, 1990, **33**, 336–344.

19 (*a*) H. Staudinger and J. Meyer, *Helv. Chim. Acta*, 1919, **2**, 635–646; (*b*) M. J. Robins and P. J. Barr, *J. Org. Chem.*, 1983, **48**, 1854–1862.

20 E. Santaniello, P. Ciuffreda and L. Alessandrini, *Synthesis*, 2005, 509–526.

21 M. Gupta and V. Nair, *Collect. Czech. Chem. Commun.*, 2006, **71**, 769–787.

22 W. L. DeLano, "*The PyMOL Molecular Graphics System*"; DeLano Scientific LLC, San Carlos, CA, USA, http://www.pymol.org.

23 CCDC-666543 contains the supplementary crystallographic data for compound **22b**. This data can be obtained free of charge from the Cambridge Crystallographic Data Centre *via* www.ccdc.cam.ac.uk/products/csd/request/.

24 F. Jeannot, G. Gosselyn, D. Strandring, M. Bryant, J.-P. Sommadossi, A. G. Loi, P. La Colla and P. Mathé, *Bioorg. Med. Chem.*, 2002, **10**, 3153–3161.

25 R. F. Schinazi, J. P. Sommadossi, V. Saalmann, D. L. Cannon, M.-W. Xie, G. C. Hart, G. A. Smith and E. F. Hahn, *Antimicrob. Agents Chemother.*, 1990, **34**, 1061–1067.

26 L. J. Stuyver, S. Lostia, M. Adams, J. Mathew, B. S. Pai, J. Grier, P. Tharnish, Y. Choi, Y. Chong, H. Choo, C. K. Chu, M. J. Otto and R. F. Schinazi, *Antimicrob. Agents Chemother.*, 2002, **46**, 3854–3860.